Distributions of Intramolecular Distances in the Reduced and Denatured States of Bovine Pancreatic Ribonuclease A. Folding Initiation Structures in the C-Terminal Portions of the Reduced Protein†

Amiel Navon,‡ Varda Ittah,‡ Pavel Landsman,‡ Harold A. Scheraga,*,§ and Elisha Haas*,‡

Faculty of Life Sciences, Bar Ilan University, Ramat Gan 52900, Israel, and Baker Laboratory of Chemistry and Chemical Biology, Cornell University, Ithaca, New York 14853-1301

Received August 16, 2000; Revised Manuscript Received October 26, 2000

ABSTRACT: The purpose of this investigation is to characterize the reduced state of RNase A (r-RNase A) in terms of (i) intramolecular distances, (ii) the sequence of formation of stable loops in the initial stages of folding, and (iii) the unfolding transitions induced by GdnHCl. This is accomplished by identifying specific subdomain structures and local and long-range interactions that direct the folding process of this protein and lead to the native fold and formation of the disulfide bonds. Eleven pairs of dispersed sites in the RNase A molecule were labeled with fluorescent donor and acceptor probes, and the distributions of intramolecular distances (IDDs) were determined by means of time-resolved dynamic nonradiative excitation energy transfer (TR-FRET) measurements. The mutants were designed to search for (a) a possible nonrandom fold of the backbone in the collapsed state and (b) possible loops stabilized by long-range interactions. It was found that, under folding conditions, (i) the labeled mutants of r-RNase A in refolding buffer (the R_N state) exhibit features of specific (nonrandom) compact but very dispersed subdomain structures (indicated by short mean distances, broad IDDs, and a weak dependence of the mean distances on segment length), (ii) the backbone fold in the C-terminal β-like portion of the molecule appears to adopt a native-like overall fold, (iii) the N-terminal α-like portion of the chain is separated from the C-terminal core by very large intramolecular distances, larger than those in the crystal structure, and (iv) perturbations by addition of GdnHCl reveal several conformational transitions in different sections of the chain. Addition of GdnHCl to the native disulfide-intact protein provided a reference state for the extent of expansion of intramolecular distances under denaturing conditions. In conclusion, r-RNase A under folding conditions (the R_N state) is poised for the final folding step(s) with a native-like trace of the chain fold but a large separation between the two subdomains which is then decreased upon introduction of three of the four native disulfide cross-links.

The kinetics of the oxidative refolding of reduced bovine pancreatic ribonuclease A (RNase A)[1] by dithiothreitol have led to a folding mechanism involving intermediate structures on several different pathways (*1*−*5*), and the structures of two of these (three-disulfide) intermediates have been determined by multidimensional NMR spectroscopy (*6*, *7*). A nonrandom distribution of one-disulfide bonds in the ensembles of intermediate species containing one (*8*) and two (*9*) disulfide bonds has been observed; similar distributions were reported by Ruoppolo et al. (*10*). Small-angle X-ray scattering (*11*−*13*) and time-resolved dynamic nonradiative excitation energy transfer (TR-FRET) (*14*−*16*) techniques have been applied to determine the overall dimensions and their distributions in denatured and partially folded states, with the conclusion that the reduced and partially folded states of RNase A are far from being able to be described as a statistical coil. Similar conclusions were deduced for reduced and denatured bovine pancreatic trypsin inhibitor (*17*, *18*). It was proposed that specific long-range interactions between pairs of single residues or short stretches of the chain prior to formation of secondary structures can be a key factor in determining the steps that direct the folding pathway (*18*). Nevertheless, information is still lacking about

† This research was supported by Grants GM-39372 and GM-24893 from the National Institutes of Health and by grants from the U.S.-Israel Binational Science Foundation and the Israel Science Foundation. This work was also supported by the National Foundation for Cancer Research.

‡ Bar Ilan University.

§ Cornell University.

[1] Abbreviations: RNase A, bovine pancreatic ribonuclease A; wt-RNase A, wild-type RNase A; W^m-RNase A, mutant RNase A with residue *m* replaced with tryptophan; (W^m,C^n)-RNase A, mutant RNase A with residue *m* replaced with tryptophan and residue *n* replaced with cysteine; Cca, 7-acetamidocoumarin-4-carboxylic acid; I-Cca, 7-iodoacetamidocoumarin-4-carboxylic acid; (*m*−*n*)-RNase A, (W^m,C^n)-RNase A labeled at residue *m* with tryptophan and at residue *n* with cysteine coupled with Cca; r-RNase A, reduced RNase A; r-(*m*−*n*)-RNase A, reduced (*m*−*n*)-RNase A; R_N, reduced form of the protein in native buffer (i.e., under folding conditions); U, disulfide-intact protein denatured in 6 M GdnHCl; GdnHCl, guanidinium hydrochloride; Ac, acetate; DMSO, dimethyl sulfoxide; DTT, dithiothreitol; EDTA, ethylenediaminetetraacetic acid; HEPES, *N*-(2-hydroxyethyl)piperazine-*N*′-2-ethanesulfonic acid; MOPS, 3-(*N*-morpholino)propanesulfonic acid; TCEP, tris(2-carboxyethylphosphine) hydrochloride; FRET, fluorescence resonance energy tranfer; TR-FRET, time-resolved dynamic nonradiative excitation energy transfer; D-experiment, measurement of the fluorescence decay of the donor in a singly labeled mutant (no acceptor); DD-experiment, measurement of the fluorescence decay of the donor in a doubly labeled mutant; fwhm, full width at half-maximum of a distribution; IDD, distribution of intramolecular distances; R_{mean}, mean of an IDD; CD, circular dichroism; HPLC, high-performance liquid chromatography; β_n, β-strand number *n*; CFIS, chain folding initiation site; EED, end-to-end distance.

10.1021/bi001946o CCC: $20.00
Published on Web 12/13/2000

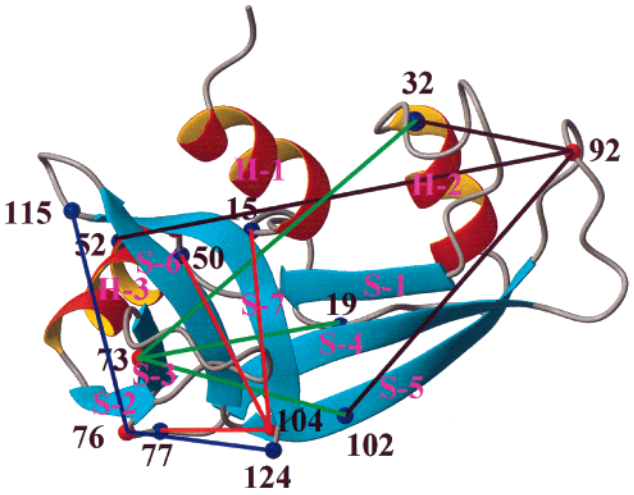

FIGURE 1: View of all the labeled mutants shown on the crystal structure of RNase A (*19*). The secondary structure segments are shown, and the α-carbons of the four inserted tryptophan residues are represented as red spheres. The α-carbons representing the nonnative cysteine residues are represented by blue spheres. Eleven colored straight lines mark the pairs of sites for which distance measurements are carried out: green for the Trp-73 mutant, blue for the Trp-76 mutant, black for the Trp-92 mutant, and red for the Trp-104 mutant. The *β*-strands are numbered S-*i* ($i = 1-7$), and the α-helices are labeled H-*i* ($i = 1-3$).

the initial *conformational* transitions of the chain as it passes from the reduced to the early intermediate forms with *part* of its full complement of disulfide bonds.

The work presented here was undertaken to acquire this information, primarily to determine how local and long-range interactions influence the conformation of the chain in its various stages of folding to the native structure. The experimental approach was based on the hypotheses that, in the partially folded state of RNase A, (a) some degree of order might be found in the ensemble of conformers that form the compact state of the molecule under folding conditions, (b) the order to be found in the ensemble can be characterized by deviation of the means and the widths of intramolecular distance distributions (IDDs) from those expected for a statistical coil state of the molecule, (c) long-range interactions can bring remote segments of the backbone together, and (d) the structural features to be found in the compact state of r-RNase under folding conditions (the R_N state) are probably related to structural elements present in the native state of the RNase A molecule; i.e., in some sections, the overall fold of the backbone resembles that of the native state.

Most methods used in the past for characterization of the chain conformation in the R_N state, and with disulfide bonds intact under denaturing conditions (the U state), provided only mean values of structural parameters, averaged over the full length of the molecules (*11*−*13*). These limitations are overcome by using the TR-FRET method, which is applied here to determine the means and widths of intramolecular distance distributions in 11 pairs of residues in mutants of the RNase A chain (Figure 1) in the R_N and U state, respectively. Each mutant contained one tryptophan residue, which served as a donor of excitation energy and a nonnative cysteine residue that was subsequently labeled with an amino-coumarin alkylation reagent, which served as an acceptor of excitation energy. The lifetimes of the excited states of the probes are on the nanosecond time scale so that conformers that exchange at rates slower than nanoseconds can be resolved, and each section of the chain is probed selectively without averaging over the whole molecule.

To reduce possible perturbation of the conformation of the chain in the partially folded state due to the effect of the mutations and the chemical labeling, only residues with side chains exposed to the solvent on the surface of the protein molecule were modified. The design was based on the extent of exposure in the crystal structure of the enzyme molecule (*19*). The residues replaced with a tryptophan residue were Tyr-73, -76, and -92 and Lys-104. Nonnative cysteine residues were also inserted, in most cases as replacements for alanine or serine residues with well-exposed side chains according to the crystal structure; these served as sites for subsequent coupling with the acceptor probe.

Formation of nonnative, stable, disulfide cross links between any one of the nonnative cysteine residues and any one of the eight native cysteine residues was a risk in this design. Therefore, only sites that are well separated from one of the native cysteine residues along the chain and are also spatially separated in the folded conformation (according to the crystal structure) were selected for mutation. Only mutants that refolded efficiently in vitro and had high specific activities were used.

The labeling plan focused on the *β*-elements in the C-terminal subdomain of the molecule (between residues 72 and 124) and on contacts between the C- and N-terminal subdomains of the molecule. Two groups of mutants were prepared. In group I, both the tryptophan and the nonnative cysteine residue were inserted in the 60-residue *β*-layer (residues 65−124) in the C-terminal portion of the chain. Group II included mutants in which one probe (the Trp residue) was in the C-terminal portion and the other (the nonnative cysteine residue) was in the 60-residue α-layer (residues 1−60) in the N-terminal portion of the chain. The IDDs obtained for all the mutants and their perturbations by denaturant show that, in the reduced state, the C-terminal subdomain of the RNase A molecule is in compact nonrandom widely distributed conformations. The N-terminal portion of the chain is widely separated from the compact C-terminal portion, and the molecule appears to have a large gap between the two termini. In a late intermediate stage of folding, this gap is closed by three of the four native disulfide bonds (*6*, *7*).

MATERIALS AND METHODS

Materials. All enzyme preparations and chemicals used in this work were purchased from Boehringer Mannheim or Sigma, unless stated otherwise.

Preparation of Doubly Labeled Fluorescent Mutants of RNase A. The production and purification of recombinant RNase A, including oligonucleotide site-directed mutagenesis, and the production and purification of recombinant RNase A mutants, are discussed in a previous paper (*20*). A single tryptophan residue (at positions 73, 76, 92, and 104, respectively) and a nonnative cysteine residue (at positions 15, 19, 32, 50, 52, 77, 102, 115, and 124, respectively) replaced single solvent-exposed residues in each mutant; these cysteines were subsequently blocked by an alkylating fluorescent reagent. The residues that were mutated were

selected by three main criteria: (a) relevance of the sites to the structural studies to be described below, (b) exposure of the side chains to the solvent, and (c) minimal perturbation of the native structure and the folding of the molecule. A set of 11 (out of a possible 36) double-site mutants was prepared in which, in addition to the insertion of a tryptophan residue, another residue was replaced with a cysteine. The RNase A mutants were expressed and purified as described previously (*20*). The product obtained after a final HPLC purification step contained one mixed disulfide between the extra (ninth, nonnative) cysteine residue and the glutathione that was used in the folding step of the purification procedure (*20*).

Selective Reduction of the Mixed Disulfide (the DTT Pulse). To reduce the extra (mixed) disulfide with glutathione selectively, and thereby expose the cysteine residue, DTT and GdnHCl were added to final concentrations of 10 mM and 0.25 M, respectively. This solution was allowed to incubate for 30 min at room temperature. The salt, the DTT, and the free glutathione were separated from the protein by gel filtration through a 15 cm × 1.5 cm G-25M Sephadex column equilibrated with 100 mM sodium acetate buffer (pH 4.0). The material from the first peak was collected, and its volume was reduced to 5 mL using an Amicon concentrator with a YM3 membrane. Under these conditions, none of the native disulfide bonds of wt-RNase A, nor those of the single-tryptophan mutants, can be reduced. In a control experiment, a test was carried out for the selectivity of the reduction of the mixed disulfide by the DTT pulse treatment; i.e., wt-RNase A was treated under the same conditions. The protein fraction that eluted from the gel filtration columns (following the DTT pulse) was tested for free thiol reactive groups by the Elman reaction which showed a complete absence of free thiols. This shows that the four native disulfide bonds could not be reduced under these conditions, and the only reactive SH group produced by this DTT treatment of the (W^m,C^n)-RNase A mutants was that of the nonnative extra cysteine residue engineered at the selected sites.

Alkylation of the Reduced Nonnative Sulfhydryl Group with a Fluorescent Reagent. The product of the gel filtration step was an RNase A mutant with a single, nonnative, sulfhydryl group. The pH of the freshly prepared (W^m,C^n)-RNase A solution was promptly changed to 8.0 by addition of 55 μL of 2 M Tris per milliliter of protein solution. This was followed by addition of an aliquot of a 0.5 M EDTA solution to a final concentration of 5 mM. 7-Iodoacetamidocoumarin-4-carboxylic acid (I-Cca) (*21*) dissolved in DMSO was immediately added to a molar ratio of 5:1 (dye:protein). The final DMSO concentration was up to 6% (v/v) depending on the initial volume of the protein sample. The reaction mixture was incubated in the dark overnight at room temperature. The mixture was then dialyzed against 100 mM sodium acetate (pH 5.0) (in the dark), and the labeled protein was purified by using cation exchange HPLC (as described for the purification of the unlabeled protein in ref *20*). The fluorescent reagents used in this study were negatively charged, and therefore, the labeled fraction eluted at lower ionic strength; hence, full separation from the unlabeled protein was achieved. The products of this preparation were doubly labeled RNase A mutants, (m−n)-RNase A, with a tryptophan that served as a donor in the FRET experiments (replacing residue m) and residue n replaced with a cysteine residue alkylated with 7-acetamidocoumarine-4-carboxylic acid (Cca).

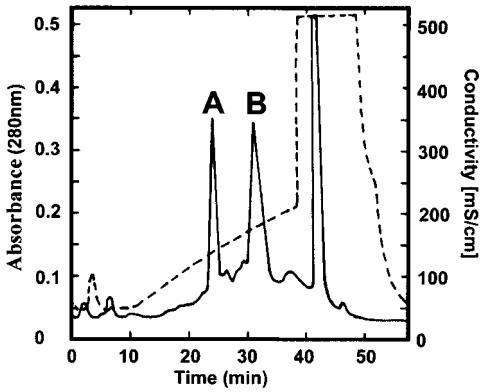

FIGURE 2: Cation exchange HPLC elution profile of (92−32)-RNase A labeled with Cca coumarin at residue 32. The labeled protein was eluted with an NaCl gradient (dashed line). The absorbance at 280 nm is represented by the solid line. A designates the coumarin-labeled (W^{92},C^{32})-RNase A, and B designates residual nonlabeled (W^{92},C^{32})-RNase A.

Table 1: Specific Activity of W^m-RNase A and (W^m,C^n)-RNase A Mutants Relative to the Activity of the Wild-Type Protein

(W^m,C^n)-RNase A mutant[a]	activity (%)[b]	(W^m,C^n)-RNase A mutant[a]	activity (%)[b]
W^{73}	92 ± 10	W^{92}	85 ± 6
W^{73}, C^{19}	80 ± 7	W^{92}, C^{32}	85 ± 5
W^{73}, C^{32}	93 ± 5	W^{92}, C^{52}	82 ± 9
W^{73}, C^{102}	90 ± 9	W^{92}, C^{102}	83 ± 5
W^{76}	86 ± 7	W^{104}	94 ± 5
W^{76}, C^{115}	84 ± 8	W^{104}, C^{15}	81 ± 11
W^{76}, C^{124}	87 ± 7	W^{104}, C^{50}	80 ± 8
		W^{104}, C^{77}	92 ± 10

[a] Each mutant protein contains one tryptophan residue (m). In some mutants, residue n was replaced with cysteine. [b] Specific activity relative to wild-type RNase A.

In principle, it is still possible that two mutations (one Trp and one Cys residue per mutant) could perturb the structures to allow a native cystine residue to react as well. This does not seem to be the case since (a) the CD and the activity measurements showed that the structural perturbations were very small, (b) it is well-known that, in the absence of denaturant, RNase A does not undergo reduction even at high DTT concentrations (*22*), and (c) in a previous paper (*20*) it was shown that the insertion of Trp residues caused only minor changes in the thermal stability of the protein. Therefore, it is reasonable to conclude that the native disulfide bonds could not react with the alkylation reagent, and that the labeling was specific at the sites selected by the insertion of the nonnative cysteine residue.

The doubly labeled mutants were purified by cation exchange HPLC. A typical separation is shown in Figure 2. This HPLC profile demonstrates that the labeled protein eluted in a well-defined fraction that was very well separated from the nonlabeled RNase A mutant. The separation is based on the negative charge of the carboxyl group of the coumarin moiety. The enzymatic activities of the labeled RNase A mutants do not differ significantly from that of the native protein (Table 1). The absorption spectra of the labeled mutants illustrated in Figure 3 (showing similar peak heights for Trp and Tyr vs coumarin) confirm that the ratio of the coumarin dye to protein was 1:1. The control experiments

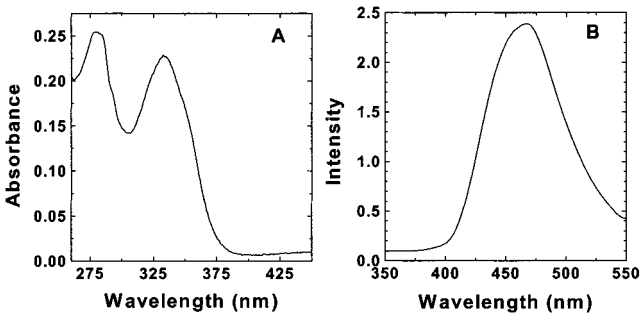

FIGURE 3: Absorption (A) and fluorescence (B) spectra of Cca-labeled (92−102)-RNase A mutant at a concentration of 0.6 mg/mL in 100 mM sodium acetate (pH 5.0) (excitation wavelength of 335 nm, bandwidth of 3.2 nm).

Table 2: Extinction Coefficients and Steady-State Anisotropy of the Single Trp Residues Inserted into the W^m-RNase A Mutants

mutant[a]	extinction coefficient (M^{-1} cm^{-1}) (278 nm)	fluorescence emission maximum (nm)	steady-state anisotropy of the tryptophan emission in the native state[b]	steady-state anisotropy of the tryptophan emission in the reduced state under native conditions
wt-RNase A	9700 ± 200			
W^{73}	13700 ± 200	334	0.22 ± 0.03	0.09 ± 0.02
W^{76}	15050 ± 200	337	0.15 ± 0.02	0.06 ± 0.01
W^{92}	14700 ± 200	332	0.17 ± 0.02	0.13 ± 0.02
W^{104}	13500 ± 130	342	0.16 ± 0.01	0.17 ± 0.02

[a] W^m-RNase A mutants. [b] Steady-state anisotropy of the tryptophan fluorescence in the native state (fourth column) or in the R_N state (last column), with an excitation wavelength of 300 nm (slit width of 2 nm) and an emission wavelength of 360 nm (slit width of 3 nm), measured at room temperature and pH 7.

and characteristics determined for the labeled mutants, viz., (a) the extinction coefficients, (b) the HPLC purity and elution volume, (c) the specific activities, (d) the absorption and emission spectra, (e) the sequences of the genes used for the production of the mutants, and (f) the absence of labeling of wild-type recombinant RNase A and of the four W^m-RNase A mutants (m = 73, 76, 92, and 104) by coumarin in the DTT-reduction-pulse control experiment, confirm the suitability of the series of labeled (W^m,C^n)-RNase A mutants for the planned study of the refolding transitions by spectroscopic methods.

Enzymatic Activity. The enzymatic activity was determined by the procedure described in ref *7*. The relative rates of catalysis, reported as a percentage of the wild-type rate, are presented in Table 1.

Determination of Extinction Coefficients. The determination of the extinction coefficients of the single tryptophan mutants in the native state is described in ref *20*, and the data are listed in Table 2. The extinction coefficient of the Cca probe attached to each of the mutant proteins was found to be 18 500 ± 500 M^{-1} cm^{-1}. This value was later used to determine the concentrations of the (m−n)-RNase A labeled mutants.

Spectroscopic Characterization of Fluorescent Probes. Absorption and fluorescence spectra were obtained as described in ref *20*. All measurements were carried out at 20 ± 0.1 °C.

The Förster distances (R_0) of the donor−acceptor pairs of the fluorescent probes (*23*, *24*) were calculated by using the spectroscopic properties of the probes, with the quantum yield q of the tryptophan in each of the mutants determined by the reference method, using a solution of degassed naphthalene in cyclohexane [q = 0.23 (*25*)] and a solution of free L-tryptophan in water [q = 0.144 (*26*)]; the same values were obtained with both reference methods. The orientation factor κ^2 was taken to be $^2/_3$, as justified by Haas et al. (*27*), and the refractive index of the medium between the probes was taken to be 1.34. The fluorescence emission spectrum of the tryptophan residue in the W^m-RNase A mutants was measured for each folding form of the mutant enzyme. This was used for calculation of the overlap integral (in R_0) for the labeled (m−n)-RNase A mutants under the corresponding folding condition. The radiative lifetime of the donor was determined from measurements of the lifetime and the quantum yield of the tryptophan residues in the mutants.

Sample Preparation. To obtain protein samples in the denatured state without reduction of the disulfides, viz., the U state, samples of wt-RNase A or RNase A mutants were prepared at a concentration of 30 μM in the presence of 6 M GdnHCl. Two buffer solutions were used, either 40 mM HEPES (pH 7.0) or 40 mM phosphate (pH 7.0), as described for each experiment.

For the preparation of protein samples for time-resolved nonradiative energy transfer experiments in the reduced state under folding conditions, viz., the R_N state, the protein was brought to a concentration of 30 μM in the presence of 7 M GdnHCl and 150 mM DTT. The protein solutions were incubated at 37 °C for 30 min and then subjected to dialysis overnight (for 8 h) against 1000 volumes of a solution of 40 mM HEPES (pH 7.0), 20 mM DTT, 5 mM EDTA, and the desired concentration of GdnHCl (0−6 M). In some experiments (indicated in the text), the HEPES buffer was replaced with 40 mM phosphate (pH 7.0), and the effect of phosphate ions on the structure of the protein was studied.

Time-Resolved Fluorescence Measurements. Measurements of fluorescence lifetimes were carried out by using the time-correlated single-photon counting system described previously (*17*, *18*). Fluorescence emission was collected through a polarizer oriented at the magic angle (≈55°) relative to the polarization of the exciting beam. Decay of fluorescence emission, $I(t)$, was analyzed by a nonlinear least-squares multiexponential fitting (*28*).

Time-Resolved Nonradiative Energy Transfer Measurement. All measurements were carried out at 22 °C and pH 7.0, unless stated otherwise, with excitation at 297 nm. Two fluorescence decay curves were recorded for each set of energy transfer experiments. These were (a) the fluorescence decay curve of the tryptophan residue in the absence of an acceptor in W^m-RNase A (the D-experiment) and (b) the fluorescence decay curve of the tryptophan residue in the presence of the acceptor attached to the engineered cysteine residue in the corresponding (m−n)-RNase A (the DD-experiment). The background emission was routinely subtracted from the corresponding fluorescence decay curves. To measure background emission, a solution of recombinant wt-RNase A was used. Donor emission was monitored at 360 nm (bandwidth of 12−16 nm). Data collection for each set of measurements (two samples) was carried out on the same day within a short time period. This reduced possible variations due to changes in the calibration of instruments.

Data Analysis. Intramolecular distance distribution (IDD) functions for each folding form of the ($m-n$)-RNase A mutants were obtained from simultaneous global analysis (*28*) of the above two-experimental fluorescence decay curves which were recorded under the respective folding conditions. Deconvolution and global analysis of the fluorescence decay curves were carried out using the Marquardt nonlinear least-squares method (*28*−*31*). Two theoretical decay curves were calculated for each set of FRET experiments and fitted to the corresponding experimental curves. The calculated decay curves were prepared by numerical solution of a modified version of a second-order differential equation (*28*, *30*), as described previously (*32*). The model function used for the analysis was

$$N(r) = 4C\pi r^2 \exp[-a(r - b)^2] \quad (1)$$

where $N(r)$ is the probability of finding the acceptor probe at a distance r from the donor, C is a normalization constant, and a and b are free parameters that determine the full width at half-maximum (fwhm) and the mean (R_{mean}) of the distribution.

The evaluations of the quality of fit obtained for each analysis and the significance of the parameters were based on five indicators: the global χ^2 values, the distributions of the residuals, the autocorrelation of the residuals, the error intervals of the calculated parameters (*28*, *30*, *32*), and the χ^2 values obtained for each DD-experiment when analyzed using a simple multiexponential decay model. The error intervals were obtained by a rigorous analysis procedure carried out for each set of experiments (*28*, *32*).

In all the analyses, best fits of the experimental data with the theoretical curves based on the calculated parameters of the IDDs were obtained when very small diffusion coefficients ($<10^{-7}$ cm^2/s) were assumed. This can in part be due to the short fluorescence lifetime of the tryptophan residues and in part to an indication of structural restrictions that dampen the conformational fluctuations of the chain segment. Accurate estimation of the small diffusion rates was not possible with the present pair of probes. Therefore, the contribution of intramolecular diffusion to the enhancement of the FRET was assumed to be negligible in the work presented here. The fine details of the IDD, e.g., the shape of the tails or the extent of skewness, cannot be resolved with confidence in the present experimental system, i.e., for the present donor−acceptor pairs and the distances spanned in the U and R_N states.

Control Experiments. To test for the absence of intermolecular energy transfer, samples containing a mixture of D and A protein species at a ratio of 1:1 were prepared at the same protein concentration that was used for the fluorescence energy transfer (FRET) experiments. The fluorescence decay of the donor in those mixtures was measured in the native and R_N states. No intermolecular energy transfer was detected.

To check that the probes were dynamically averaged (to justify use of a κ^2 value of $^2/_3$), the steady-state anisotropy or the anisotropy decay of the fluorescence of the tryptophan residues (in W^m-RNase A mutants) and those of the acceptor [in ($m-n$)-RNase A] were measured. Measurements of anisotropy decay of the tryptophan residues were carried out as described in ref *33*, using Glan-Thomson polarizers. The anisotropy decay of the acceptor was measured by using a Ti-sapphire system, with excitation at 450 nm, in the laboratory of E. Pines at Ben Gurion University (Ben Gurion, Israel). Each anisotropy decay, $r(t)$, was analyzed by multiexponential decay according to the following equation:

$$r(t) = \sum_{i=1}^{M} \beta_i \exp(-t/\phi_2) \quad (2)$$

where β_is and ϕ_is are the amplitudes and rotational correlation times, respectively.

RESULTS

(1) Preparation and Characterization of the Series of Singly Labeled Trp Mutants of RNase A. The HPLC profiles, the CD spectra (*20*), the thermal transitions, and the high specific activity levels of the mutants (*20*) confirm that possible perturbations of the native structure and its stability due to the mutations were very limited. These experiments show that the Trp mutants of RNase A designed and produced here are native-like and are suitable for studies of unfolding and refolding of the RNase A molecule. Indeed, since the aim of this study is primarily the study of the nonnative states of the protein, it is reasonable to assume that the effects of the possible small structural perturbations on the results of the energy transfer experiments are even smaller.

Table 3 shows the results of measurements of the time-resolved anisotropy decay of the tryptophan fluorescence in W^m-RNase A (m = 73, 76, 92, and 104) mutants in the reduced state. Each mutant showed anisotropy decay components that reflect fast rotational freedom both locally and in the whole molecule.

(2) Preparation and Characterization of the Doubly Labeled RNase A Mutants. The DTT Pulse. Each of the four mutants, W^m-RNase A (m = 73, 76, 92, and 104), was further mutated by replacement of one residue with a (nonnative) cysteine residue. Eleven pairs of residues were prepared in two groups. Group I included pairs of residues in which both labeling sites were in the C-terminal β-layer portion of the chain (residues 65−124). In group II mutants, one probe (the Trp residue) was located in the C-terminal portion of the chain while the nonnative cysteine residue was inserted in the N-terminal α-layer portion of the chain (residues 1−60). Labeling of the nonnative cysteine residue in each of these mutants by an acceptor of excitation energy enabled determination of 11 intramolecular distance distributions (IDDs) defined by this labeling plan. These pairs are shown in Figure 1.

To assess the rotational freedom of the coumarin probe, the anisotropy decay of this probe attached to five of the extra cysteine residues of the doubly labeled mutants was measured in the native state. The results are shown in Table 3.

(3) GdnHCl-Induced Transitions; Steady-State Fluorescence Energy Transfer. As a typical example of folding−unfolding transitions, Figure 4 shows the emission spectra of r-(104−77)-RNase A at increasing concentrations of GdnHCl. The increase of the intensity of the tryptophan emission band at 360 nm with increasing GdnHCl concentra-

Table 3: Time-Resolved Anisotropy and Fluorescence Decay Data[a] for the Coumarin and the Tryptophan Residues Attached to Various Sites in the RNase A Molecules in the Native and Reduced States at Room Temperature and pH 7

mutant[b]	χ^2 [c]	τ_{av} [d] (ns)	$\tau_1(\alpha_1)$ (ns)[e]	$\tau_2(\alpha_2)$ (ns)[e]	$\tau_3(\alpha_3)$ (ns)[e]	$\phi_1(\beta_1)$ (ns)[f]	$\phi_2(\beta_2)$ (ns)[f]
coumarin dye[g]	1.27	0.59	0.063 (0.40)	0.40 (0.25)	1.33 (0.35)	0.119 (0.33)	
W^{73}, C^{19}	1.65	0.82	0.17 (0.16)	0.66 (0.46)	1.28 (0.38)	0.72 (0.14)	8.9 (0.14)
W^{73}, C^{32}	1.16	0.38	0.057 (0.42)	0.30 (0.35)	1.09 (0.23)	0.97 (0.20)	6.4 (0.088)
W^{73}, C^{102}	2.21	1.18	0.059 (0.12)	0.87 (0.50)	1.93 (0.38)		2.34 (0.195)
W^{92}, C^{32}	1.18	0.37	0.053 (0.42)	0.30 (0.36)	1.09 (0.22)	1.06 (0.20)	6.66 (0.058)
W^{92}, C^{52}	1.16	0.40	0.08 (0.49)	0.44 (0.31)	1.13 (0.20)	1.03 (0.20)	
W^{92}, C^{102}	2.41	1.08	0.058 (0.17)	0.83 (0.49)	1.95 (0.34)		2.55 (0.18)
W^{104}, C^{77}	1.56	0.45	0.075 (0.54)	0.55 (0.26)	1.32 (0.20)	0.52 (0.19)	
				Tryptophan Emission			
free Trp[h]	1.35	2.1	0.28 (0.21)	2.58 (0.79)		0.06 (0.24)	
W^{73}	1.37	1.39	0.47 (0.43)	3.51 (0.09)	1.81 (0.48)	0.71 (0.08)	>10 (0.08)
W^{76}	1.32	1.42	0.46 (0.41)	3.79 (0.11)	1.70 (0.48)	1.18 (0.12)	>10 (0.02)
W^{92}	1.30	1.29	0.38 (0.51)	3.14 (0.15)	1.83 (0.34)	0.92 (0.09)	>10 (0.122)
W^{104}	1.16	1.43	0.36 (0.46)	1.83 (0.41)	3.97 (0.13)	0.74 (0.11)	>10 (0.15)

[a] The lower four rows give the fluorescence parameters for the emission of tryptophan residues in RNase A in the reduced state. The upper rows give the same parameters for Cca attached to cysteine residues in RNase A in the native state. [b] (W^m, C^n)-RNase A mutant proteins labeled by the Cca probe at the cysteine residues n. [c] The χ^2 value for the best fit of the anisotropy data. [d] $\tau_{av} = \Sigma\ \alpha_i\tau_i/\Sigma\alpha_i$ is the mean fluorescence lifetime. [e] Fluorescence lifetime components, with the un-normalized preexponential factors given in parentheses. [f] The anisotropy correlation times according to eq 2; the uncertainty range is 25% for the short component, ϕ_1, and its associated β value, and 40% for the component ϕ_2 and β_2. [g] The free reagent Cca, not attached to a protein. [h] Tryptophan in solution at 23 °C.

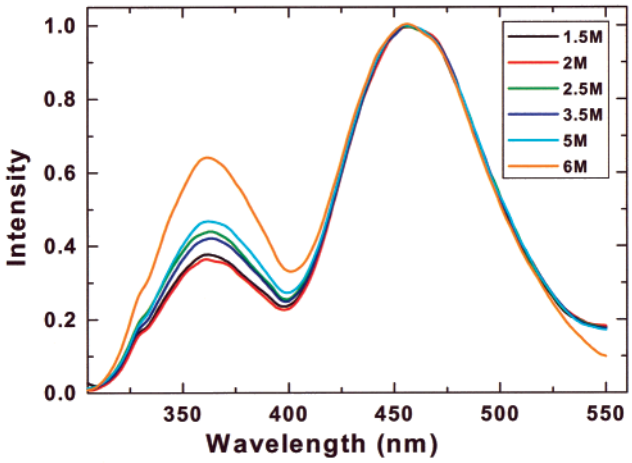

FIGURE 4: Emission spectrum of reduced (104−77)-RNase A at increasing GdnHCl concentrations at 22 °C and pH 7.0. (104−77)-RNase A (0.6 mg/mL) was reduced in the presence of 7 M GdnHCl, 50 mM HEPES (pH 7.0), and 150 mM DTT. Aliquots (200 μL) were dialyzed against the specified GdnHCl concentration in the presence of 20 mM DTT. The samples were filtered, and the fluorescence emission spectra were recorded with an excitation wavelength of 297 nm. The spectra were normalized at ~454 nm, the emission maximum of the coumarin probe.

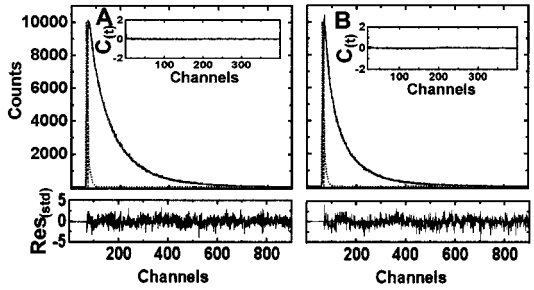

FIGURE 5: (A) Fluorescence decay curves for the tryptophan residue in W^{76}-RNase A (the D-experiment) and (B) the fluorescence decay of the tryptophan residue in (76−124)-RNase A in the R_N state in 40 mM phosphate buffer (pH 7.0) and 20 mM DTT (the DD-experiment) at room temperature. The excitation wavelength was 297 nm with emission at 360 nm (bandwidth for emission of 2 nm): (···) the system response to the excitation pulse, (- - -) the experimental trace of the tryptophan fluorescence pulse, and (—) the best fit theoretical curves obtained by the global analysis. The DD-experiment was fit to a theoretical curve based on the distribution of distances (*31*). The residuals of the fits (Res) are shown in the lower blocks, and the autocorrelation functions of the residuals [$C(t)$] are presented for each curve in the upper right inset. The χ^2 obtained in this experiment was 2.02.

tion is a clear indication of a conformational transition. The full information content of the experiment is available in the time-resolved experiments (Figure 5).

(4) Time-Resolved Experiments for RNase A in the Reduced (R_N) and Denatured (U) States. Time-resolved dynamic nonradiative excitation energy transfer was assessed using the singly and doubly labeled fluorescent protein mutants, the W^m-RNase A (donor without acceptor), and the (W^m,C^n)-RNase A doubly labeled mutants labeled at residue n by the coumarin reagent [($m-n$)-RNase A]. The measurements were carried out under two equilibrium conditions: first, under denaturing conditions, in 6 M GdnHCl with the disulfide cross-links intact (the U state), and second, under reducing but folding conditions, where the disulfide cross-links were reduced (the R_N state).

Resolution of the trace of the decay of the fluorescence of the tryptophan residues in each of the four W^m-RNase A (m = 73, 76, 92, and 104) mutants showed three components, which are attributed solely to the emission from the single tryptophan residue in each mutant. Because the excitation wavelength was 297 nm and the emission wavelength was 360 nm, the contributions from tyrosine residues were negligible. In a control experiment, a sample of wild-type RNase A was tested for fluorescence emission under these excitation and emission wavelengths, but no measurable signal was detected.

The intramolecular distance distributions between the tryptophan donor and the Cca acceptor in each mutant were determined by global analysis (*28*) of the fluorescence decay of the tryptophan residues, measured under identical instrumental conditions for pairs of mutants: first in the W^m-RNase A mutant (the D-experiment) and then in the corresponding ($m-n$)-RNase A mutant (the DD-experiment) where m was

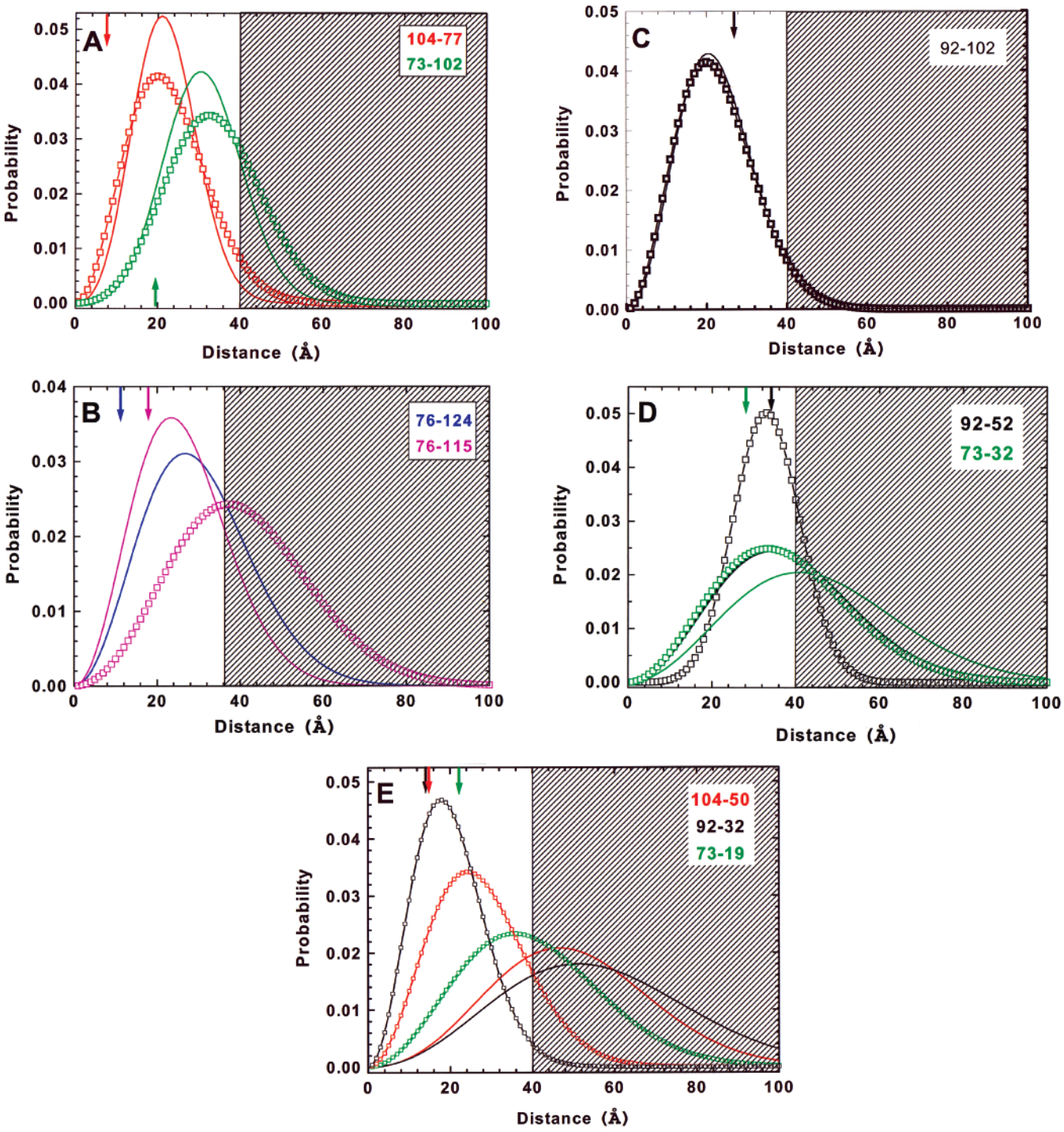

FIGURE 6: Intramolecular distance distributions at room temperature and pH 7 obtained for doubly labeled (*m*−*n*)-RNase A mutants in the R_N and U states. The fluorescence decay of the tryptophan residue in each mutant protein was measured in 40 mM HEPES buffer (pH 7) containing 20 mM DDT and 5 mM EDTA for the reduced mutants (the R_N state) (—) and for the same mutants denatured without reduction of the disulfide bonds (the U state) (□). (These distances include an approximately 3 Å contribution from the probes and the linker.) The arrows denote the distance between the C^α atoms of the labeled residues in each mutant calculated from the crystal structure. The dashed areas above 40 Å designate the distance range in which the pair of probes, tryptophan-Cca, cannot be used for accurate distance measurements: (A) (104−77)-RNase A and (73−102)-RNase A, (B) (76−124)-RNase A and (76−115)-RNase A in 40 mM phosphate buffer (pH 7.0) instead of the HEPES buffer, (C) (92−102)-RNase A, (D) (92−52)-RNase A and (73−32)-RNase A, and (E) (92−32)-RNase A, (73−19)-RNase A, and (104−50)-RNase A (the IDD of the last mutant could not be calculated in the U state due to the low transfer efficiency). Data for (104−15)-RNase A are not presented because the transfer efficiency was very low, making it impossible to estimate a lower limit of the distance, even approximately.

identical for both experiments. The results are presented in Figures 5−10 and Tables 4 and 5.

An example of a data set obtained in a typical time-resolved FRET experiment and the fit to the theoretical model by the global analysis procedure is shown in Figure 5 for samples of W^{76}-RNase A and (76−124)-RNase A in the R_N state. Figure 5A shows the fluorescence decay of the donor in the absence of an acceptor; for W^{76}-RNase A in the R_N state, the average lifetime was 1.67 ns. Figure 5B shows the enhanced rate of fluorescence decay of this donor probe in

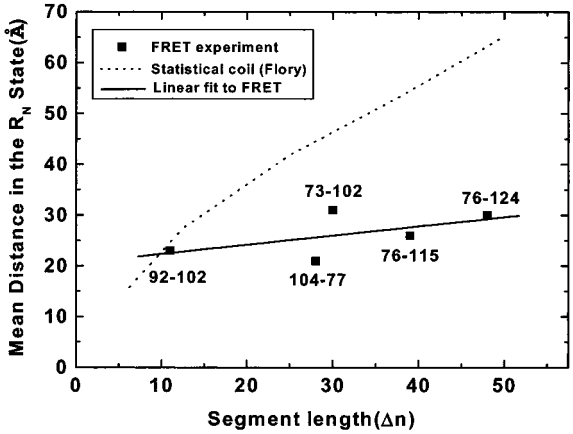

FIGURE 7: Values of R_{mean} of the IDD obtained for group I mutants with disulfides reduced under otherwise folding conditions (the R_N state) as a function of the number of residues in the labeled segments. The upper trace (dashed) shows the lower limit estimation of the expected rms end-to-end distance for a polypeptide in a statistical coil state according to Flory (*34*).

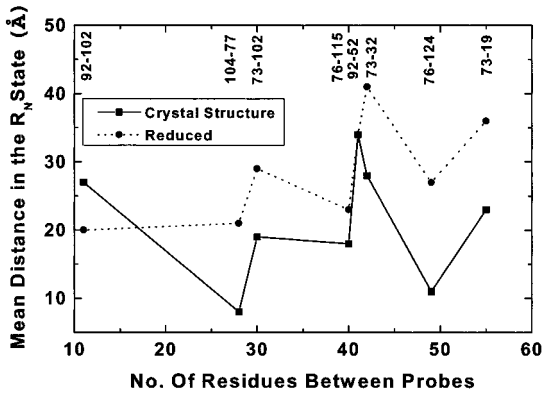

FIGURE 8: Values of R_{mean} of the IDDs obtained for group I and group IIa [and (W^{73},C^{19})-RNase A] mutants with disulfides reduced under folding conditions (the R_N state) as a function of the number of backbone residues that separate the two labeled sites in each mutant (upper trace, dashed) compared with the separation of the corresponding C^α atoms determined from the crystal structure (lower trace).

the presence of an acceptor attached to residue 124. In this case, the average lifetime was reduced to 0.79 ns, due to excitation energy transfer.

(5) Intramolecular Distance Distributions. The means and widths of the IDDs, obtained in the R_N and U states, are shown in Tables 4 and 5, and the distributions are shown in Figure 6A−E. In Table 5 and Figure 6, the means of the IDDs of each pair of sites in the R_N and U states are compared with the corresponding $C^\alpha-C^\alpha$ distances of the crystal structure (*19*) and, in Figure 7, with the mean distance predicted for a polypeptide of the same length in a statistical coil conformation (*34*) (no entry is given in Figure 6 for residues 104−15 because of the large value of R_{mean}). This comparison was made in a search for native-like features of the backbone fold of the protein in the R_N state.

The TR-FRET experiment reports the distances between the two transition dipole moments of the probes. Therefore, the calculated IDDs are only apparent distributions; the values of R_{mean} determined in these experiments were expected to be 3 ± 2 Å larger than the corresponding $C^\alpha-C^\alpha$ distances, due to the contribution of the size of the probes and the linkers. In the U state, the disulfide bonds cross-link labeled segments and restrict the distances between the labeled sites. An "effective segment length", Δn, is thus defined as the number of residues between two labeled sites from two different chain segments cross-linked by a disulfide bond. The IDDs obtained in the U state are used as references for the disordered state of chain segments in a good solvent.

(6) Dependence of R_{mean} of the IDDs on Segment Length, Determined in the Reduced State. Figure 7 shows the mean of the IDDs of the group I mutants in the R_N state as a function of the number of residues in the labeled segments. The values of R_{mean} predicted for polypeptide chains in the statistical coil state (*34*) are also shown. This figure clearly shows that *there is very little dependence of the values of R_{mean} on the chain length*. Figure 7 thus shows that (a) the C-terminal section of the chain is compact and not in a statistical coil conformation and (b) there should be some sort of order in the compact state of the chain which is not randomly collapsed.

Figure 8 shows the same data for a larger group of mutants, and in addition, the corresponding $C^\alpha-C^\alpha$ distances determined from the crystal structure (*19*) are shown for comparison. This figure demonstrates a strong correlation between the distances measured in the crystal structure and those measured using the time-resolved FRET in the R_N state. The two graphs show very similar patterns of variation. (The differences vary between 8 and 19 Å.) This correlation clearly demonstrates a nonrandom compaction in the R_N state and a trend of native-like chain fold.

In the group II mutants, the acceptor probe was attached to residues located in the N-terminal α-layer half of the chain while the donor was in the C-terminal *β*-layer subdomain. The mutants (73−32)-RNase A and (92−52)-RNase A [group IIa (Table 5)] showed a similar pattern but with values of R_{mean} in the R_N state larger than the $C^\alpha-C^\alpha$ distances in the crystal structures. These are chain segments of 42 and 41 residues with mean distances larger than those measured for the 40- and 49-residue segments of the C-terminal subdomain [mutants (76−115)-RNase A and (76−124)-RNase A, respectively]. The mutants of group IIb (pairs 92−32, 104−15, and 104−50), for which Δn is ≥55 residues, showed much larger differences between the inter-residue distances determined in the crystal structure and the mean distances determined in the R_N state. In the R_N state, the means of these IDDs were larger than the range for which significant distance determination with the present pair of probes could be made; therefore, only a lower limit of R_{mean} was estimated.

This series of values of mean distances within the molecule of RNase A in the R_N state is the first evidence that, in this state, the β- and α-layer portions of the backbone of the molecule are separated by large distances in solution, while the β-layer portion is compact but with a nonrandom folding of the backbone (corresponding experiments for probing the distances within the N-terminal α-layer portion are planned).

(7) Specific Characterization of IDDs of Groups of Mutants. The following is a detailed analysis of the IDDs for each chain segment, and comparison with the distances determined from the crystal structure and possible distances for a randomly collapsed polypeptide chain.

(7A) Group I Mutants, the C-Terminal Subdomain. (i) Mutants (104−77)-RNase A and (73−102)-RNase A: The

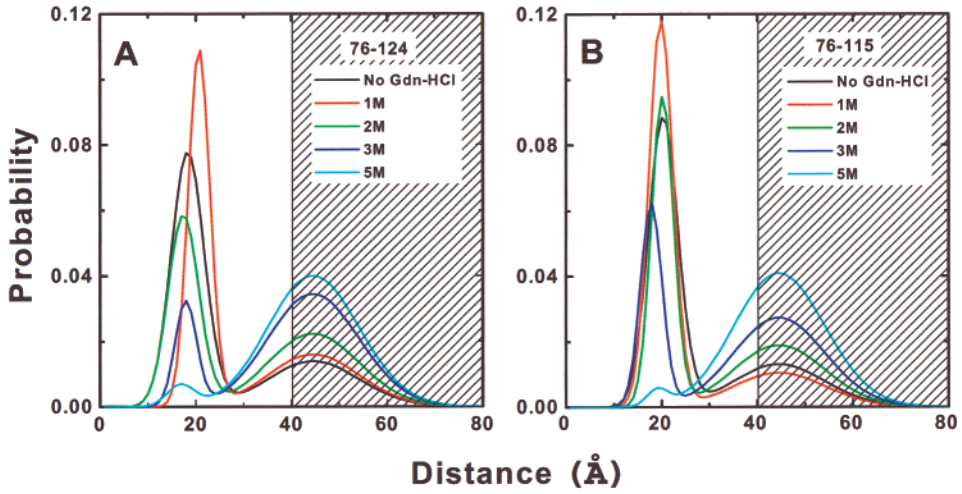

FIGURE 9: IDD of reduced (76−124)-RNase A (A) and (76−115)-RNase A (B) in the R_N state in 40 mM HEPES buffer (pH 7.0), 20 mM DTT, and 5 mM EDTA with increasing concentrations of GdnHCl. A model of two subpopulations was used for the global analysis. The mean and width of the second subpopulation was fixed at 40 Å, representing a fraction of the molecules with an expanded conformation. The shape of the IDD of this subpopulation could not be determined with the present pair of probes, and the only meaningful value is the size of the population. The parameters of the first subpopulation were determined by the global analysis. As the concentration of GdnHCl was increased, from 0 to 6 M, the proportion of the two subpopulations increased from 30 to 95%.

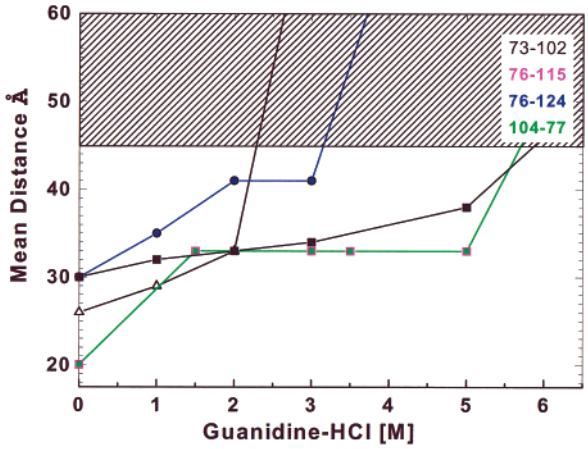

FIGURE 10: R_{mean} of the IDDs of four doubly labeled RNase A mutants in the reduced state as a function of GdnHCl concentrations. (76−115)-RNase A (pink trace) and (76−124)-RNase A (blue trace) were reduced and transferred into the R_N state in phosphate buffer, while (104−77)-RNase A (green trace) and (73−102)-RNase A (black trace) were in HEPES buffer. The transition to large distances, beyond the range of significant determination with the present pair of probes (shaded region), occurred at different GdnHCl concentrations for each mutant.

28- and 30-Residue Portion of Strands β4 and β5. The mutants (104−77)-RNase A and (73−102)-RNase A enclose a segment of 28 and 30 residues, respectively, in the C-terminal portion of the chain. This is a chain segment that, in the crystal structure, forms β-strands 4 and 5 in a closed loop. Figure 6A shows that the corresponding R_{mean} values obtained for the R_N and U states were comparable and 13 and 12 Å larger than the $C^\alpha-C^\alpha$ distances in the crystal structure (which includes a possible 3 ± 2 Å contribution from the size of the probes and the linker).

(ii) Mutants (76−124)-RNase A and (76−115)-RNase A: The Extended C-Terminal Segment. In a first series of TR-FRET measurements, the two mutants (76−124)-RNase A and (76−115)-RNase A were dissolved in phosphate buffer (in the R_N state). Figure 6B shows corresponding R_{mean} values of 30 and 26 Å, respectively, with large fwhm values. In the U state, where the effective chain lengths are reduced to 28 and 19 residues, respectively, the transfer efficiencies dropped to less than 10%. These low transfer efficiencies indicate a large expansion of the molecular volume.

In the second series of TR-FRET experiments, (76−124)-RNase A and (76−115)-RNase were dissolved in HEPES buffer instead of the phosphate buffer. Under these conditions, the donor fluorescence decay curves could not be fit with a model of a single wide IDD function. A model of at least two distinct subpopulations (Figure 9), one with a native-like R_{mean} and small width and the second with a very large R_{mean}, gave satisfactory fits. For both IDDs, the fraction of the subpopulation characterized by the shorter mean distance (native-like) was ca. 70% at 22 °C. A gradual reduction of the fraction of the first subpopulation (with short R_{mean} values) and a corresponding increase in the size of the second subpopulation was induced by increasing concentrations of GdnHCl (Figure 9). This appears to be a transition between two states of these segments of the polypeptide chain. The midpoint of the transition for both mutants was between 2 and 3 M GdnHCl. These results show that, in the C-terminal section of the chain, a weakly stabilized chain fold with native-like features is formed in the R_N state. It is in equilibrium with the unfolded state, and the equilibrium depends on the solvent composition and the temperature. This fold can be in the form of a long loop stabilized by a hydrophobic core which involves nonpolar patches of a few residues from the two ends and other sections of this polypeptide stretch.

(iii) Mutant (92−102)-RNase A: The Segment That Forms β-Strand 5. In the crystal structure, the 11-residue segment from residue 92 to residue 102 forms one strand of the antiparallel β-structure (strand 5) and a β-turn (Figure 1). This is the shortest segment labeled in the present series. Figure 6C shows that, in the R_N state, the mean of the distribution of distances between the two ends of this segment

Table 4: Results of the Time-Resolved Excitation Transfer Experiments and Parameters of the Respective IDDs Obtained for the r-(*m*−*n*)-RNase A Mutants in the R_N State (reduced under folding conditions at room temperature and pH 7)

group	mutant[a]	R_0[b] (Å)	τ_{av}(donor)[c] (ns)	τ_{DA}[d] (ns)	donor q[e]	a[f]	b[f]	R_{mean} (Å)[g]	fwhm (Å)[h]	χ^2[i]
I	W^{73}, C^{102}	23.2	1.1	0.81	0.1	23.0	0.0044	31	22.5	1.36
								30.2−31.6	19.0−27.6	
	W^{76}, C^{115}	24.2	1.67	0.8	0.11	0.0052	0.0019	26.2	26.6	1.67
								25.5−26.3	25.5−26.6	
	W^{76}, C^{124}	24.1	1.67	0.79	0.11	0.009	0.0014	30.2	31.4	2.02
								30.2−35.7	29.5−37.0	
	W^{92}, C^{102}	24.3	1.58	0.89	0.13	4.27	0.003	23.0	23.0	1.36
								22.6−25.2	18.2−26.6	
	W^{104}, C^{77}	23.5	1.32	0.69	0.13	0.059	0.003	20.6	21.3	1.44
								20.6−25.5	19.4−26.1	
IIa	W^{73}, C^{32}	23.2	1.1	0.83	0.08	0.0002	0.0006	>40	>40	1.41
	W^{92}, C^{52}	24.3	1.58	1.14	0.13	2.0	0.009	38.5	39.5	1.3
								38.5−43.1	31.4−44.5	
IIb	W^{73}, C^{19}	23.2	1.1	0.83	0.08	0.880	0.0008	40	40	1.18
								38.1−45.6	31.7−47.5	
	W^{92}, C^{32}	24.3	1.58	1.19	0.13	12.0	0.0005	>40	>40	1.41
	W^{104}, C^{15}	24.3	1.35	1.35	0.13			>40	>40	
	W^{104}, C^{50}	24.3	1.35	1.25	0.13	19.78	0.0008	>40	>40	1.96

[a] (*m*−*n*)-RNase A mutant labeled with a Cca probe at residue *n*. [b] The Förster critical distance calculated for each derivative under solution conditions of the R_N state. [c] Average fluorescence lifetime of the donor in the absence of an acceptor (the D-experiment); $\tau_{av} = \Sigma\alpha_i\tau_i/\Sigma\alpha_i$. [d] Average fluorescence lifetime of the donor in the presence of the acceptor attached to residue *n* (the DD-experiment). [e] The fluorescence quantum yield of the donor in the absence of an acceptor. [f] The parameters of the model distribution function used for the analysis of the fluorescence decay curves (eq 1). [g] The mean of the IDD, and the range. [h] Full width at half-maximum of the IDD and the range. [i] The global χ^2.

Table 5: Mean and fwhm of the Distributions of Intramolecular Distances in the Labeled RNase A Mutant Molecules in the R_N and U States at 22 °C and pH 7

group	mutant[a]	segment length Δn[b]	effective segment length[c]	$C^\alpha-C^\alpha$ distance from the crystal structure[d] (Å)	R_{mean} in the R_N state[e] (Å)	fwhm (Å)	mean distance in the U state[f] (Å)	fwhm (Å)	estimation of the mean EED in the statistical coil state[g] (Å)
I	W^{73}, C^{102}	30	19	20	31	22	34	28	42
	W^{76}, C^{115}	40	19	18	26	27	>40	39	49
	W^{76}, C^{124}	49	28	11	30	31	>40		54
	W^{92}, C^{102}	11		27	23	23	23	23	18
	W^{104}, C^{77}	28	21	8	21	21	23	23	41
IIa	W^{73}, C^{32}	42	19	28	>40	>44	38	39	50
	W^{92}, C^{52}	41	17	35	38	39	33	19	50
IIb	W^{73}, C^{19}	55	20	23	40	40	>40	42	57
	W^{92}, C^{32}	61	13	15	>40	>40	20	20	60
	W^{104}, C^{15}	90	33	17	>40		>40		73
	W^{104}, C^{50}	55	16	15	>40		>24	29	57

[a] The two residues that were labeled; the first (m) is the tryptophan residue, the second (n) is the cysteine labeled by the Cca acceptor. [b] Number of residues in the backbone chain segment whose ends are the labeled residues. [c] The number of residues in the chain segment of minimal length which is created by cross-linking by two cysteine residues. The disulfide bond is counted as another residue. [d] The distance between C^α atoms of residues *m* and *n* according to PDB entry 7RSA. [e] Mean of the IDD determined under folding conditions in the reduced state. [f] Mean of the IDD determined in 6 M GdnHCl for the disulfide-intact RNase A (the U state). [g] Theoretical estimation of the mean distance between the ends of a polypeptide chain of an equivalent chain length (Δn) in a statistical coil state.

(23 Å) is *smaller* than the distance found in the crystal structure (27 Å, Table 5).

(7B) Group II Mutants: Intramolecular Distances between Residues in the C-Terminal Chain β-Layer and Helices 1−3 in the N-Terminal α-Layer of the Chain. (i) Group IIa: Probing Distances across the Active Site Cleft. (a) Mutant (73−32)-RNase A. In the crystal structure, residues 73 and 32 appear on two opposite sides of the folded RNase A molecule with a large separation of 27 Å between the α-carbons of these two residues. Therefore, this distance depends on the compactness of the molecule, i.e., on the distance between helix II and the C-terminal hydrophobic core and on the folding of the 42-residue segment enclosed between these two residues (Figure 1). Table 5 and Figure 6D show that, in the reduced state, the transfer efficiency was low, and the calculated mean of the IDD had only limited statistical significance. There is no evidence for any deviation from a random distribution of distances.

(b) Mutant (92−52)-RNase A. The results obtained for (92−52)-RNase A are quite different from those for (73−32)-RNase A, although the segment length is about the same. In the R_N state, R_{mean} was increased by only ∼10% relative to the $C^\alpha-C^\alpha$ distance in the crystal, and the fwhm was very large.

(ii) Group IIb: The Distance between Residues in the N-Terminal α-Layer of the Chain and Residues in the C-Terminal β-Subdomain. (a) Mutants (104−50)-RNase A, (104−15)-RNase A, (92−32)-RNase A, and (73−19)-RNase A. These four mutants were designed to probe the compactness of the molecule in the R_N state by measurements of the IDDs of long chain segments connecting the two structured layers of the chain. For each of them, the observed

transfer efficiencies were very low, and a reliable determination of the parameters of the IDD with the present pair of probes was not possible. It is possible that the mean distances were close to a separation expected for a statistical coil state. *These results show that, in the R_N state, the interactions between the N- and C-terminal portions of the chain are very limited and the separation is large, perhaps to the extent of separation as in a statistical coil state.*

(8) Further Characterization of the Structure of the Reduced State of RNase A. Denaturant-Induced Unfolding of the C-Terminal Subdomain of RNase A in the R_N State. The variation of the means of several IDDs with increasing concentrations of GdnHCl is shown in Figure 10. Two minor transitions could be observed for the chain section of residues 104−77, one between 0 and 1.5 M GdnHCl and a second one at >5 M GdnHCl. The R_{mean} values of the 40- and 49-residue segments of reduced mutants (76−115)-RNase A and (76−124)-RNase A, respectively, in phosphate buffer, show a gradual increase up to 2 M GdnHCl at 22 °C (Figure 10). At >2 M GdnHCl, a sharp drop of the transfer efficiencies occurred at two different denaturant concentrations. This means that different parts of the C-terminal section have different GdnHCl transitions, i.e., different stabilities.

The transfer efficiencies were measured for a few labeled mutants in the reduced state in 6 M GdnHCl. Seven mutants showed transfer efficiencies close to zero, which corresponds to a large shift of the IDD to the range of distances larger than 40 Å. Two mutants, (104−77)-RNase A and (73−102)-RNase A, in which the labeled segment length was less than 31 residues, showed very low, but non-zero, transfer efficiencies even under the extreme denaturing conditions. When the length of these two labeled segments (28 and 30 residues) is considered, it is not surprising (because of the widths of the distributions) that, even in a statistical coil state, a fraction of the molecules could be in the distance range that allows efficient transfer of excitation energy. The short chain segment labeled in mutant (92−102)-RNase A (11 residues) shows a high transfer efficiency (30%) under these conditions, and the corresponding calculated IDD had an R_{mean} of 35 Å.

These observations show that the denaturant-induced expansion of the dimensions of the chain is not a nonspecific effect of solvation of a randomly collapsed chain but rather a stepwise breaking of specific subdomain structures.

(9) Summary of Results. The above results provide the following information about the state of the RNase A molecule in the absence of the network of disulfide cross-links in the R_N state.

In the reduced RNase A molecule, the widths of almost all the IDDs that were determined in the present series of experiments were very large, as expected for ensembles of unordered chain molecules. This means that the local interactions that stabilize the secondary structures are not effective enough under these conditions to stabilize local structural elements. These observations show that the chain appears to be at least locally unfolded, while the mean distances indicate that some very weak long-range interactions lead to partial order on a larger scale.

Several features of the current results summarized below support the hypotheses underlying the present work:

(a) In the R_N state, the C-terminal subdomain is in a compact conformation. Some chain sections have mean distances closer to the corresponding $C^{\alpha}-C^{\alpha}$ distance determined in the crystal structure [e.g., R_{mean} of 38 Å for the IDD of the mutant (92−52)-RNase A]. Very weak chain length dependence of the mean distances and its pattern indicate that the chain is not randomly collapsed.

(b) Unlike the other labeled segments, the short chain segment between residues 92 and 102 is in a stretched conformation (R_{mean} = 23 Å, shorter than the 27 Å of the crystal structure, but larger than that of a statistical coil, ∼19 Å) not only in the R_N state but also in the U state where R_{mean} was also 23 Å. The C-terminal chain sections (residues 76−124 and 76−115) in HEPES buffer exhibited clear evidence for an equilibrium of two subpopulations, one with a native-like R_{mean} and one with a much larger segmental end-to-end distance.

(c) At least three nonoverlapping segmental transitions were observed in the GdnHCl-induced denaturation of reduced RNase A.

(d) Group II mutants showed large R_{mean} values.

DISCUSSION

(1) Considerations Pertaining to the Data Analysis and the Quality of Fits. The goal of the present experiments was to search for the low-resolution overall conformational trends of the protein backbone in the reduced state under folding conditions. To that end, a large number of doubly labeled mutant protein variants had to be prepared. This was made possible by using the natural probe (tryptophan) as a donor. The use of tryptophan as a donor in time-resolved FRET experiments involves difficulties which limit the resolution of the experiments. These include short fluorescence lifetime, multiexponential decay of the fluorescence, local interactions with the protein environment, and possible limited dynamic averaging. In the reduced state, the last two sources of uncertainty are considerably reduced. The effect of local interactions on the donor fluorescence lifetimes was taken into account by using the fluorescence lifetime of Trp in each mutant determined in the absence of an acceptor under the conditions used for the FRET experiment. The extent of dynamic averaging of the orientations of the probes was estimated using fluorescence anisotropy decay measurements (see the discussion in the Supporting Information).

James et al. (*35*) used tryptophan 140 in staphylococcal nuclease as a donor and presented a detailed discussion of the uncertainties associated with that probe. The four Trp residues used in the present study are surface residues, and the anisotropy measurements show that their rotational freedom is larger than that for Trp-140 of staphylococal nuclease. Following the same arguments made by James et al., the data presented in Table 3 (and Table III in ref *27*) lead to the conclusion that the calculated uncertainty of R_0 and the width of the calculated IDDs is less than 10%.

A detailed discussion of the mode of analysis of experiments similar to those used here was presented by Ittah and Haas (*18*), and is relevant to the present experiments as well. Since the fluorescence decay of the donor in the absence of an acceptor is not monoexponential, the mode of analysis described by Sinev et al. (*33*) was used. In this analysis, the variation of R_0 with the rate of fluorescence decay of the donor was taken into account.

(2) Chain Dimensions in the R_N State. Each physical method averages a distribution of conformations with

somewhat different weights. The present method was developed for more direct determination of the parameters of the IDDs, and it gives less weight to the extreme distances. Sosnik and Trewhella (*11*) used small-angle X-ray scattering and deduced that reduced RNase A has a radius of gyration, R_g, of 19 Å. Nöppert et al. (*12*) used dynamic light scattering and CD measurements to determine the compactness and residual secondary structure of RNase A, reduced and denatured by 6 M GdnHCl. They found that reduction of all disulfides led to total unfolding and that further increases in temperature had no additional effect on the dimensions. For reduced RNase A at 20 °C, they reported a Stokes radius of 29.1 ± 0.6 Å at pH 4.0, which was increased to 31.4 ± 0.6 Å by addition of 6 M GdnHCl. The calculated R_g was 50.0 ± 1.0 Å for reduced denatured RNase A, which is larger than that expected for an ideal random coil at the θ point, according to Miller and Goebel (*36*). These results led the authors to conclude that reduced and denatured RNase A is not in a compact state. Zhou et al. (*13*) used synchrotron radiation for small-angle X-ray scattering and reported an R_g value of 20 Å for reduced RNase A in 50 mM Tris buffer (pH 8.1) containing 20 mM DTT. Using the approximation derived for infinite chain length, the root-mean-square end-to-end distance (*34*) would thus be 49 Å. These authors deduced that, in the R_N state, RNase A is in neither a random coil nor a compact denatured state. Miller and Goebel (*36*) calculated dimensions of unperturbed random coil polypeptides which, when applied to RNase A, led to a root-mean-square end-to-end distance of 110 ± 5 Å.

All of these results were based on averaging data collected simultaneously from all sections of the chain. The calculation of a radius implicitly assumes a spherical shape of the molecule. The results presented here show that this is not a correct approximation. The pair of probes used in this study provides distances that are limited to a range smaller than the full dimensions of the molecule; therefore, direct comparison with the results of the scattering and hydrodynamic methods is limited. The mean distances that could be determined did not exceed the lower limit suggested for the overall diameter of the molecule. In this respect, it is of interest to note that, in the R_N state, group IIa mutant (92−52)-RNase A ($\Delta n = 41$), which was designed for measurement of the diameter of the molecule in one direction (see Figure 1), had an R_{mean} value of 38 Å (not including the contribution of the linkers, the corresponding $C^\alpha-C^\alpha$ distances in the crystal structures was 34 Å). This can be taken as a rough approximation of one mean dimension of the molecule. The second dimension to be measured by group IIb mutants was much larger.

(3) C-Terminal Subdomain. In the crystal structure, the 49-residue C-terminal section of the chain (residues 76−124) is 73% β-structure, and forms two antiparallel β-sheet structures (Figure 1). Its two ends are close to each other, and it forms part of a hydrophobic cluster (with only 11 Å between the α-carbons of residues 76 and 124 in the crystal structure). The mutant (76−115)-RNase A contains a shorter, 40-residue section of the same chain segment, which lacks the β-structure between residues 115 and 124 (strand S-7).

The mean distances between the ends of five segments of the chain in the C-terminal part of the RNase A molecule in the R_N state lack a clear correlation with Δn, the segment lengths (see Table 5). *The large widths of the distributions show that the ensemble of populated conformations is very dispersed, i.e., that the interactions that are responsible for the bias of the ensemble from a compact disordered conformation are very weak.* One possible interpretation is that, in the R_N state, the backbone segment that forms β-strands 4 and 5 (Figure 1) tends to form a loop shape, and the ends of the segment are held together loosely in a hydrophobic core formed in the C-terminal subdomain of the molecule.

Taken together, the five IDDs (of Figure 6A−C) determined within the 52-residue C-terminal segment of RNase A in the R_N state show that the C-terminal subdomain of the molecule forms an ensemble of compact loosely folded conformations with native-like features. Similar results were obtained for sperm whale apomyoglobin by M. Jamin, J. Dyson, and P. E. Wright (private communication), who showed the presence of native-like structure in the unfolded state.

(4) Intramolecular Distances between Residues in the C-Terminal β-Layer and the N-Terminal α-Layer of the Chain. The results presented here emphasize the importance of spatial variability of the conformational states in subdomains of the molecule. The large distances between the C- and N-terminal sections of the chain show an extended nonspherical shape of the ensemble. This information is missed when the chain dimensions are averaged. Given the mean distances, it is possible to calculate an approximate characteristic ratio (*34*) for the chain segments in the R_N state. Damaschun et al. (*37*) calculated a characteristic ratio (R_{mean}/nl^2, where n is 104 and l is 0.38 nm) of 8.43 for acid-denatured apocytochrome *c* which they considered to be in a random coil state. In a statistical coil state, one can expect an approximately uniform characteristic ratio for all sections of the polypeptide chain. The fact that the characteristic ratio calculated from the R_{mean} of most of the IDDs obtained in this study was considerably smaller and varied between 1.09 and 3.3 is additional evidence for the nonrandomness of the chain conformations.

(5) Effect of Phosphate Ions on the Conformation of RNase A in the Reduced State. Clearly, the phosphate buffer used in the experiment in Figure 6B induced a conformational change which reduced the difference between these two subpopulations, and therefore, a single-component IDD could be used to represent the end-to-end distances of these two C-terminal chain segments. Figure 11shows how phosphate ion can interact with residues His-12, His-119, and Lys-41. Phosphate ions also affect the kinetics of oxidative folding of reduced RNase A, but by a nonspecific effect, rather than the specific binding shown in Figure 11 (*38*).

The crystal structure shows that, besides the nonspecific binding effect (*38*), residues 12, 41, and 119 can interact with phosphate ions (*19*) and thus cross-link three sections of the chain (see Figure 11) and increase the compactness of the whole molecule. This can reduce the difference between the two subpopulations so that the experimental data can fit one widely dispersed ensemble of molecules. This "substrate-dependent stablization of the native-like chain fold by cross-linking" enhances the folding in a manner reminiscent of the role of the disulfide cross-links in folding.

(6) Disulfide Bonds in RNase A Fasten the N-Terminal Portion of the Chain to the C-Terminal Hydrophobic Core. Three out of four disulfide bonds in the RNase A molecule

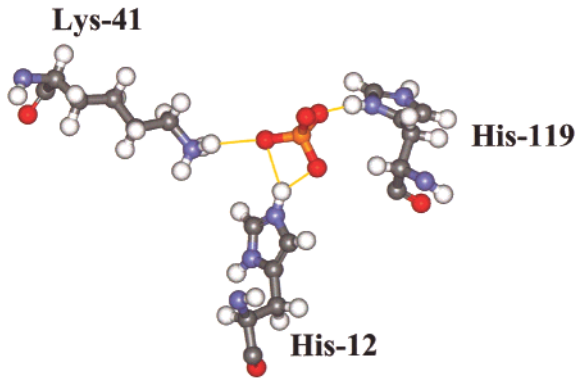

FIGURE 11: Three residues that interact with the phosphoryl group in the active site of RNase A and thus effectively cross-link three chain segments. The coordinates for this drawing were taken from the crystal structure of a complex of RNase A with a phosphate ion (PDB entry 5RSA).

cross-link widely separated residues. These are the 26−84, 58−110, and 40−95 pairs. These three long-range disulfide bonds bridge gaps of 59, 53, and 56 residues, respectively, a very uniform separation. In each of them, one residue is in the N-terminal half of the molecule and the second is in the C-terminal half of the chain. It seems that a major contribution of the disulfides to the folding of the molecule is closure of the cleft between the N-terminal α-layer and the C-terminal *β*-layer of the molecule. The stabilization of the interaction between the subdomains seems to be essential for stabilization of the native secondary and tertiary structure in the whole molecule, including the C-terminal subdomain. In the U state, the disulfides stabilize the compact structure of the molecule both by reduction of the segment lengths and by closure of the cleft between the two parts of the molecule.

RNase A thus appears to be divided into two very distinct folding subdomains, the N-terminal α-subdomain and the C-terminal *β*-subdomain (*39*). Interestingly, the fourth disulfide (Cys-65−Cys-72), which appears to form preferentially upon oxidation of the reduced form (*8*), stabilizes the bend of the chain in a section that connects the two subdomains of the molecule. The NMR structures of analogues of the three-disulfide folding intermediates des-(65−72)-RNase A (*6*) and des-(40−95)-RNase A (*7*) show that, at this three-disulfide stage, the native structure is formed and that the fourth disulfide is necessary to remove the slight degree of flexibility that is present at the three-disulfide stage. Comparison of Figures 1 and 12 shows the relation between the locations of the disulfide bonds and the Trp residues.

The above results and discussion suggest a few additional conclusions about reduced RNase A in the R_N state: (a) In the absence of secondary structure, the loose folding of the C-terminal subdomain can lead to loops that can be precursors for the native *β*-structures. (b) Weak long-range interactions seem to be involved in the folding of this subdomain. In particular, there are possible hydrophobic interactions between residues in the following segments: 78−80, 104−107, and 116−124. These can be chain-folding initiation structures, as proposed by Matheson and Scheraga (*40*). (c) The main contribution of the disulfide bonds is the closure of the structural gap between the two subdomains of the chain and compaction of the molecule as one unit of two closely

FIGURE 12: Diagram of native RNase A showing the location of the four disulfide bonds (*19*).

packed α- and *β*-layers. The attachment of the N-terminal chain elements to a "template" formed by the C-terminal chain section can supply additional long-range interactions that contribute the missing stability of the secondary structures in both subdomains. (d) The overall contour of the ensemble of conformers is probably very elongated. (e) These experiments show the strength of the present experimental approach, and emphasize the advantage of using a series of predesigned pairwise-labeled mutants for TR-FRET experiments.

The current data show the power of the present approach in dissecting the folding transition of complex protein molecules. Additional planned experiments (pertaining to distances within the N-terminal portion) of the kind presented here will enable further detailed examination of the present hypothesis that chain segments form loops that are poised for formation of the native secondary structure elements of the native chain fold.

ACKNOWLEDGMENT

We are indebted to Dr. W. J. Wedemeyer for helpful comments on the manuscript.

SUPPORTING INFORMATION AVAILABLE

Some details relating to the Results and Discussion. This material is available free of charge via the Internet at http://pubs.acs.org.

REFERENCES

1. Rothwarf, D. M., Li, Y.-J., and Scheraga, H. A. (1998) *Biochemistry 37*, 3760−3766.
2. Rothwarf, D. M., Li, Y.-J., and Scheraga, H. A. (1998) *Biochemistry 37*, 3767−3776.
3. Iwaoka, M., Juminaga D., and Scheraga, H. A. (1998) *Biochemistry 37*, 4490−4501.
4. Xu, X., and Scheraga, H. A. (1998) *Biochemistry 37*, 7561−7571.
5. Welker, E., Narayan, M., Volles, M. J., and Scheraga, H. A. (1999) *FEBS Lett. 460*, 477−479.
6. Shimotakahara, S., Rios, C. B., Laity, J. H., Zimmerman, D. E., Scheraga, H. A., and Montelione, G. T. (1997) *Biochemistry 36*, 6915−6929.

7. Laity, J. H., Lester, C. C., Shimotakahara, S., Zimmerman, D. E., Montelione, G. T., and Scheraga, H. A. (1997) *Biochemistry 36*, 12683−12699.
8. Xu, X., Rothwarf, D. M., and Scheraga, H. A. (1996) *Biochemistry 35*, 6406−6417.
9. Volles, M. J., Xu, X., and Scheraga, H. A. (1999) *Biochemistry 38*, 7284−7293.
10. Ruoppolo, M., Torella, C., Kanda, F., Panico, M., Pucci, P., Marino, G., and Morris, H. R. (1996) *Folding Des. 1*, 381−390.
11. Sosnick, T. R., and Trewhella, J. (1992) *Biochemistry 31*, 8329−8335.
12. Nöppert, A., Gast, K., Muller-Frohne, M., Zirwer, D., and Damaschun, G. (1996) *FEBS Lett. 380*, 179−182.
13. Zhou, Y., Vitkup, D., and Karplus, M. (1999) *J. Mol. Biol. 285*, 1371−1375.
14. McWherter, C. A., Haas, E., Leed, A. R., and Scheraga, H. A. (1986) *Biochemistry 25*, 1951−1963.
15. Beals, J. M., Haas, E., Krausz, S., and Scheraga, H. A. (1991) *Biochemistry 30*, 7680−7692.
16. Buckler, D. R., Haas, E., and Scheraga, H. A. (1995) *Biochemistry 34*, 15965−15978.
17. Gottfried, D. S., and Haas, E. (1992) *Biochemistry 31*, 12353−12362.
18. Ittah, V., and Haas, E. (1995) *Biochemistry 34*, 4493−4506.
19. Wlodawer, A., Svensson, L. A., Sjölin, L., and Gilliland, G. L. (1988) *Biochemistry 27*, 2705−2717.
20. Navon, A., Ittah, V., Laity, J. H., Scheraga, H. A., Haas, E., and Gussakovsky, E. E. (2001) *Biochemistry 40*, 93−104.
21. Sinev, M., Landsmann, P., Sineva, E., Ittah, V., and Haas, E. (2000) *Bioconjugate Chem. 11*, 352−362.
22. Li, Y.-J., Rothwarf, D. M., and Scheraga, H. A. (1995) *Nat. Struct. Biol. 2*, 489−494.
23. Förster, Th. (1948) *Ann. Phys. (Leipzig) 2*, 55−75.
24. Van der Meer, B. W., Cooker, G., III, and Chen, S. Y. S. (1994) *Resonance Energy Transfer Theory and Data*, p 150, VCH Publishers, New York.
25. Berelman, I. B. (1971) *Handbook of Fluorescence Spectra of Aromatic Molecules*, 2nd ed., Academic Press, New York.
26. Wiget, P., and Luisi, P. L. (1978) *Biopolymers 17*, 167−180.
27. Haas, E., Katchalski-Katzir, E., and Steinberg, I. Z. (1978) *Biochemistry 17*, 5064−5070.
28. Beechem, J. M., and Haas, E. (1989) *Biophys. J. 55*, 1225−1236.
29. Grinvald, A., and Steinberg, I. Z. (1974) *Anal. Biochem. 59*, 583−598.
30. Haas, E., Katchalski-Katzir, E., and Steinberg, I. Z. (1978) *Biopolymers 17*, 11−31.
31. Haas, E. (1996) *IEEE J. Sel. Top. Quantum Electron. 2*, 1088−1106.
32. Haran, G., Haas, E., Szpikowska, B. K., and Mas, M. T. (1992) *Proc. Natl. Acad. Sci. U.S.A. 89*, 11764−11768.
33. Sinev, M. A., Sineva, E. V., Ittah, V., and Haas, E. (1996) *Biochemistry 35*, 6425−6437.
34. Flory, P. J. (1969) *Statistical Mechanics of Chain Molecules*, Interscience, New York.
35. James, E., Wu, P. G., Stites, W., and Brand, L. (1992) *Biochemistry 31*, 10217−10225.
36. Miller, W. G., and Goebel, C. V. (1968) *Biochemistry 7*, 3925−3935.
37. Damaschun, G., Damaschun, H., Gast, K., Gernat, C., and Zirwer, D. (1991) *Biochim. Biophys. Acta 1078*, 289−295.
38. Low, L. K., Shin, H.-C., Narayan, M., Wedemeyer, W. J., and Scheraga, H. A. (2000) *FEBS Lett. 472*, 67−72.
39. Wedemeyer, W. J., Welker, E., Narayan, M., and Scheraga, H. A. (2000) *Biochemistry 39*, 4207−4216. Erratum, *39*, 7302.
40. Matheson, R. R., Jr., and Scheraga, H. A. (1978) *Macromolecules 11*, 819−829.

BI001946O